Volume 40 http://acousticalsociety.org/

International Conference on Underwater Acoustics

9 September 2020

Session 1A: Ambient Noise

Low-frequency ocean acoustics – measurements from the Lofoten-Vesterålen Ocean Observatory, Norway

Shaula Garibbo and **Philippe Blondel**,
Department of Physics, University of Bath, Bath, Somerset, BA2 7AY, UNITED KINGDOM; sg2340@bath.ac.uk; pyspb@bath.ac.uk;

Gary Heald
DSTL: Defence Scientific and Technology Laboratory, Salisbury, Wiltshire, *SP4 6GZ, UNITED KINGDOM; GJHEALD@mail.dstl.gov.uk*

Ross Heyburn
AWE Blacknest, Aldermaston, Reading, RG7 4PR, UNITED KINGDOM; ross@blacknest.gov.uk

Alan Hunter
Department of Electronic Engineering, University of Bath, Bath, Somerset, BA2 7AY, UNITED KINGDOM; ajh210@bath.ac.uk

Duncan Williams
DSTL: Defence Scientific and Technology Laboratory, Salisbury, Wiltshire, SP4 6GZ, UNITED KINGDOM; DPWILLIAMS@dstl.gov.uk

This paper will focus on acoustic measurements from the Vesterålen cabled ocean observatory, located 15 km offshore northern Norway, at a depth of 255 m. The measurements were made with a calibrated Ocean Sonic hydrophone SB35-ETH, recording since 2013. The hydrophone node is located in a large (ca. 15 km) canyon, not far from shipping lanes. We have measured acoustic variability up to the third-octave band centered on 125 Hz, the second shipping band identified in the European Marine Strategic Framework Directive (MSFD). Time scales from months (spanning several seasons across 2018) to hours have been investigated, considering broadband Source Pressure Levels (SPL, between 1--125 Hz), SPLs over 1-Hz frequency bands (to identify variability within third-octave bands and associate them with potential sources), and percentile contributions over the different frequency bands. Sounds from shipping and fin whale vocalisations are important contributors. Early analyses show it is also possible to detect sounds from far-away earthquakes apparently propagating in the water column (e.g. an m_b = 4.9 event in the Jan Mayen Fracture Zone, 830 km away), and other noise sources over ranges of up to 2212 km.

Published by the Acoustical Society of America

 https://doi.org/10.1121/2.0001324

INTRODUCTION

Sounds dominate the oceans, spanning all frequencies and coming from different sources: natural (e.g. wind, rain), biological (e.g. marine mammals, fish) and anthropogenic (e.g. ships, seismic exploration). Very-low frequency hydroacoustic signals ($<$ 100 Hz) are often associated with geophysical processes, like earthquakes and landslides, but they can be linked to man-made activities, like offshore industry, fish blasting, or even nuclear test explosions. Understanding the mechanisms generating noise below 100 Hz, has important applications for monitoring nuclear explosions (for example, the combined use of seismic, hydroacoustic and infrasound signals to detect and study distant phenomena, particularly explosions, but also submarine accidents or aircraft impacts), and to naval operations such as anti-submarine warfare, where noise can be either or both a source of interference and a source of opportunity. Current understanding of these mechanisms is very limited for noise below 100 Hz and the ocean acoustic phenomena below 10 Hz are rarely studied and even less well understood. Very often, the strong background noise will include several distinct sources, some of which can be very close and others louder but propagating from very large ranges, up to ocean-scale. It is therefore very important to understand the key acoustic signatures of these processes, along with their extreme spatial and temporal variability. The measuring and resolving power of ocean observatories can be harnessed to investigate low-frequency ambient noise over long timescales, and in a variety of background noise conditions.

DATA AND PROCESSING

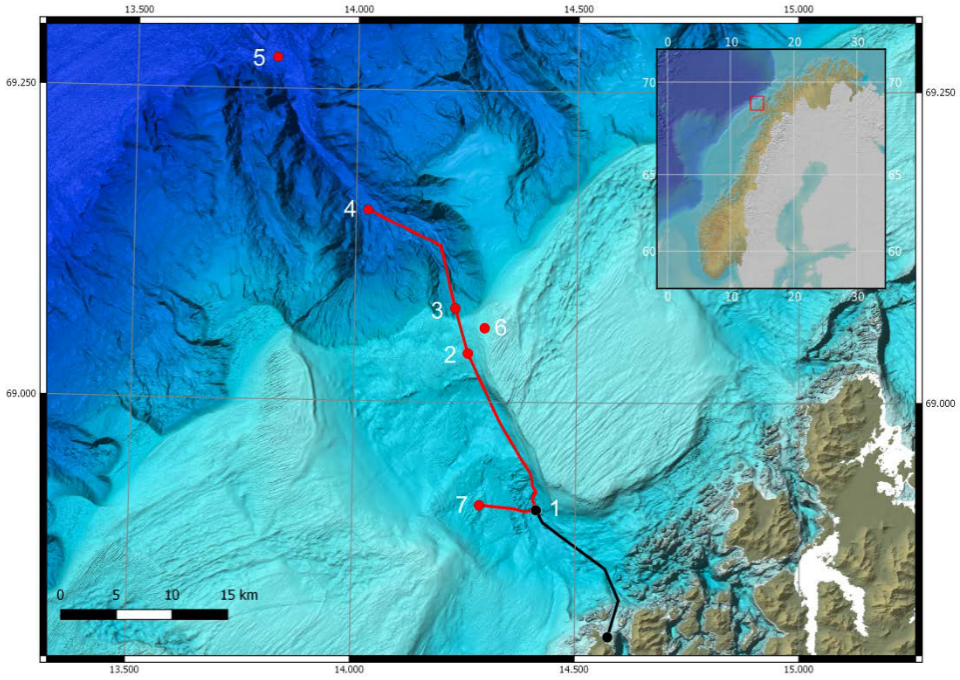

Figure 1: Layout of LoVe observatory offshore of the Lofoten Islands (insert shows the location offshore northern Norway marked with a red box); numbers 1 to 7 are used to label hydrophone nodes.[26]

The data presented here is taken from the Lofoten-Vesterålen (LoVe) observatory (Fig. 1), which is located approximately 15 km offshore of the Lofoten Islands, at a depth of 255 m on the continental shelf.[26] It is situated within the Hola Trough - one of many troughs formed during the last glaciation - and hosts

cold water coral reefs, sandwave fields, and glacigenic deposits.[5,29,31] The hydrophone (a calibrated Ocean Sonic SB35 ETH) records between 10 Hz and 200 kHz, and is mounted approximately 0.5 m above the seabed on a metallic structure which is anchored into the seabed.[23]

The data was processed using a Matlab software called PAMGuide, which performs calibrated signal processing on passive acoustic data in both terrestrial and aquatic environments.[22] The calibration parameters were taken from the Ocean Sonic hydrophone specifications,[23] and compared to previous work done at LoVe.[26]

OBSERVATIONS

WHALE VOCALISATIONS

The most commonly found whale vocalisation in the LoVe dataset is attributed to the fin whale, and is known as the "20 Hz call".[6,27] An example of this call is shown in Fig. 2. The global distribution of fin whales mean that this high amplitude, and long-propagating call is a common feature of the world's ocean soundscape.[24] It is thought to be a call made by male fin whales during breeding season to attract females from great distances[2,24] as unlike other whales, fin whales do not gather in specific areas to mate.[10]

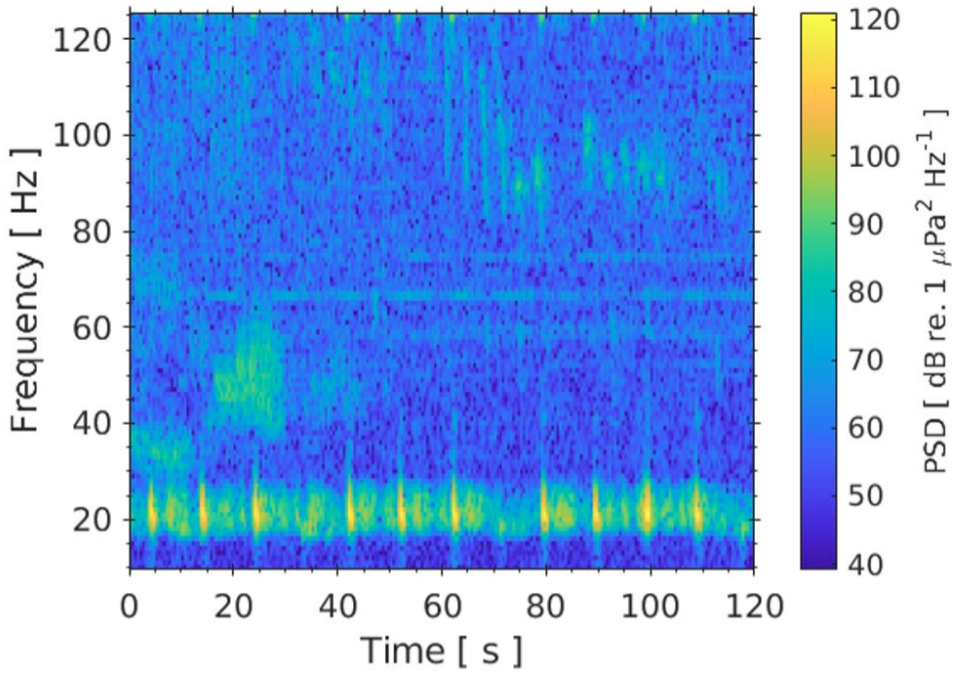

Figure 2: Example 20 Hz fin whale call observed in the LoVe data, with duration approx. 1 s at intervals of approx. 10 s, together with two groups of higher frequency vocalisations.

The 20 Hz calls are approximately 1 s in duration, consist of a frequency down-sweep between approximately 25 Hz and 17 Hz,[24] and are separated by an interval between 9 s and 34 s.[6] This is sometimes accompanied by a higher frequency up-sweep of variable bandwidth - an example of which is shown in Fig. 2. Two groups of higher frequency vocalisations are seen in the LoVe data - one that appears between 40 Hz and 80 Hz, and another that appears between approximately 80 Hz and somewhere upward of 125 Hz, which could suggest that these are recordings of two different pods.

SHIPPING

Shipping noise is generally acknowledged to be one of the two largest contributors to sound in the ocean under 1000 Hz.[13,33] Accordingly, shipping noise is observed on every day of available data from the LoVe observatory, ranging from continuous shipping noise over the course of a day, to short blips of shipping noise that are only minutes in duration. The abundance of shipping noise is most likely due to activity along a main shipping lane, located approximately 55 km northwest of the LoVe observatory, as well as lots of local shipping traffic in the form of ferries and fishing vessels.

The most distinguishable feature of shipping noise is bold, horizontal tonal lines, as shown in Fig. 3. These are attributed to propeller blade cavitation,[21] and also internal mechanisms like the engine, pumps, and generators.[32] The frequencies at which the shipping noise dominates has been found to be dependent on vessel type, load, speed, and also aspects like propeller type and hull design.[21]

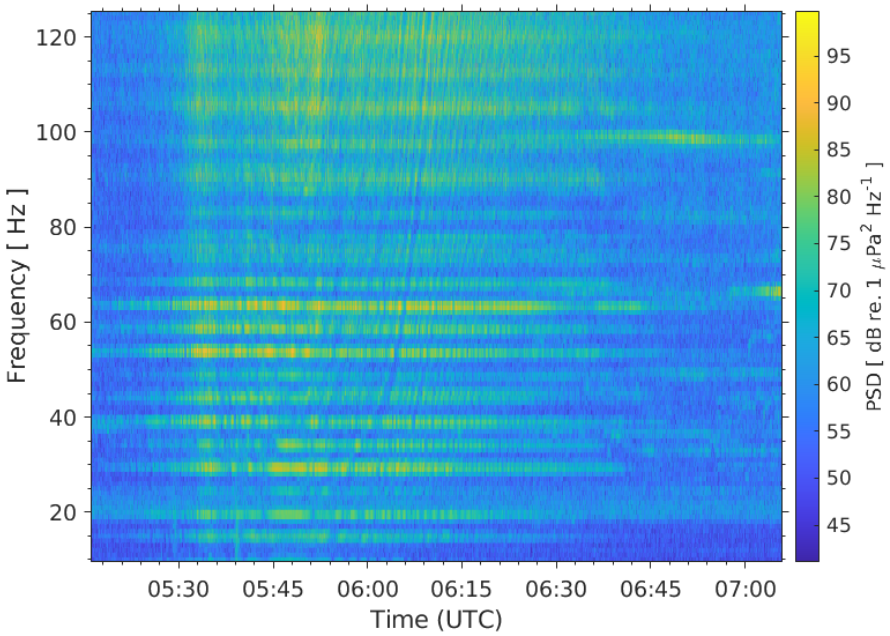

Figure 3: Example tonal lines and Lloyd's Mirror Effect from shipping noise observed in the LoVe data.

In addition to these tonal lines, another common feature of shipping noise is an upward 'U' pattern.[1,32,35] This is Lloyd's Mirror Effect (LME) - the result of interference between the direct and indirect sound propagation paths as the source point moves. The significance of this pattern is that it can be used, in conjunction with the tonal lines, to trace the source of the shipping noise,[35,36] and that the minima of these patterns represents the Closest Point of Approach (CPA) to the recording instrument.[37] In Fig. 3, one can see that the CPA of the vessel occurs at approximately 05:46 UTC (corresponding to the minima of the upward 'U' pattern).

WIND

Weather generates and influences sound in the ocean through several mechanisms - such as wave formation, radiative heat transfer, through the formation of sea ice, and many more.[34] For frequencies below 500 Hz, wind largely generates noise by forcing the surface of the ocean, leading to the formation of surface gravity waves.[20,34] The interactions between surface waves travelling in different directions generate

sound at twice the frequency of the surface wave, but only leads to insonification of the far-field if the surface waves have wave numbers of similar magnitude and are travelling in near-opposite directions, creating standing waves.[7] Over the entire year 2018, there were 33 manually-found instances of "white-out" of the spectrograms, where all frequencies between 10 Hz and 125 Hz were saturated. These instances all coincided with periods of higher wind speeds or local storms, but not all periods of high wind speeds coincided with a period of higher broadband noise.

EARTHQUAKES

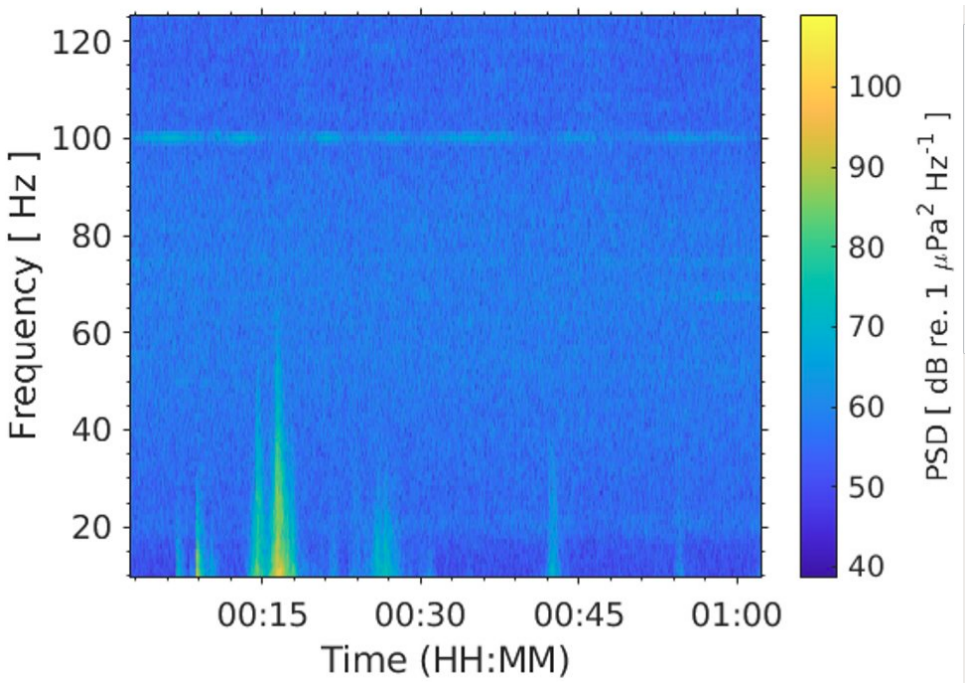

Figure 4: Signals from two earthquakes off the coast of Jan Mayen on 25/04/2018 observed in the LoVe data.

Another common signal in the LoVe dataset comes from earthquakes. These signals appear as vertical spikes along the bottom of the spectrogram - see Fig. 4. On the 25th April 2018, the International Seismological Centre (ISC) bulletin recorded an earthquake at 00:05:06 UTC of magnitude (m_b) 3.4, and another earthquake at 00:06:56 UTC of magnitude (m_b) 4.9.[18] The epicenters for both earthquakes were approximately 88 km southeast of Jan Mayen, 830 km away from the LoVe observatory. Assuming the speed of sound through seawater is 1500 $m.s^{-1}$, an approximate travel time through the water column would be 9.2 minutes, giving an Expected Time of Arrival (ETA) of 00:16:08 UTC for the larger of the two earthquakes. The largest spike signal in Fig.4 occurs at 00:16:10 UTC, within 0.5% of the predicted travel time.

In addition to the sound that travels through the water column, a portion of the sound of the earthquake travels through the solid Earth, and radiates back into the water column closer to the LoVe hydrophone node. These signals, the seismic phases, are the source of the other spike signals visible in Fig. 4 before and after the main arrival. Hydrophones commonly detect P-waves and teleseismic waves from earthquakes,[3,12,30] and in total, 62 seismic events were found in the LoVe data in 2018.

ANALYSIS

WIND

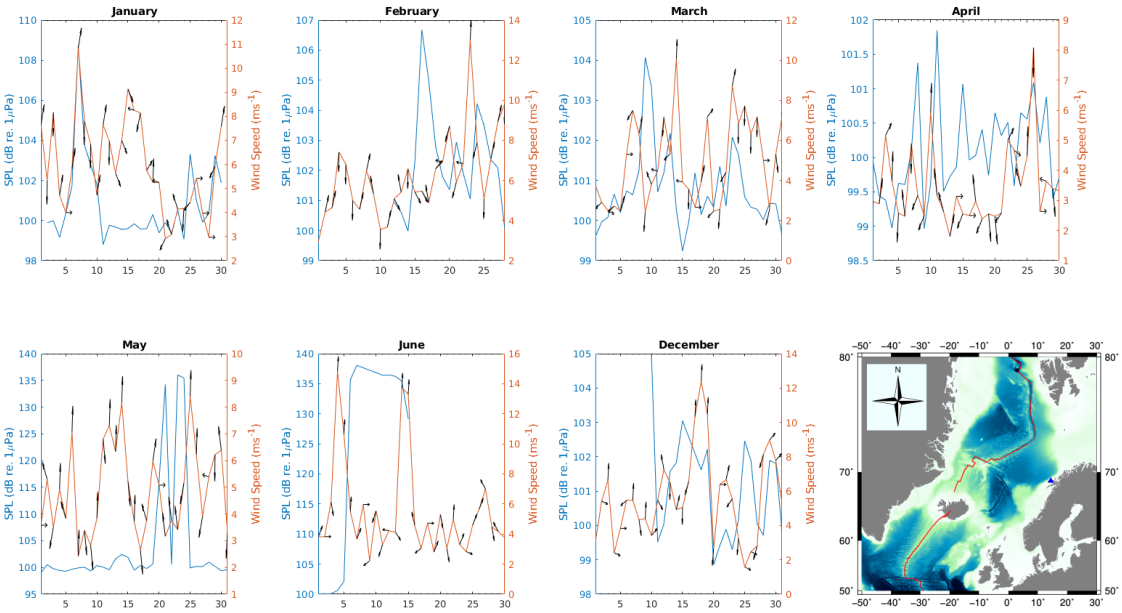

Figure 5: Acoustic effects of wind direction, tiny arrows show wind direction

Periods of high wind speeds near the LoVe observatory sometimes coincide with a "white-out" of the spectrogram, and other times, there is no signal to be seen, and no increase in broadband sound pressure level - as can be seen in Fig. 5). For example, from the 6th to the 7th January the wind blew in a NNE direction, rising by 5 m.s^{-1} over the 24-hour period. This coincided with a 7 dB increase in broadband SPL. Comparatively, during the 24-hour period between the 12th to 13th May the wind also blew in a NNE direction, rising by 1.83 m.s^{-1} and coinciding with a 2.9 dB increase in broadband SPL. Wind speed alone can only be used to crudely estimate the amount of noise transmitted underwater, as factors like duration of wind, fetch, constancy, and its direction in relation to local swells and currents, and nearby topography.[8,33] Previous work done in other areas of shallow water suggests that a wind speed threshold of approximately 10 m.s^{-1} generally has to be exceeded to cause significant changes in mean sound levels,[16] but there is also a strong site-dependence for wind-driven noise, depending on factors like ocean bottom properties, water depth, and sound-speed profiles.[17,28]

EARTHQUAKES

An arbitrary area was selected around LoVe primarily to minimise the size of the ISC earthquake bulletin to be manually checked against the LoVe data to 1090 earthquakes, from what would have been hundreds of thousands. The area was also selected as it included a variety of potential geophysical acoustic sources - for example, glaciers in Greenland and Svalbard, the Mid-Atlantic Ridge, and volcanic activity in Iceland.

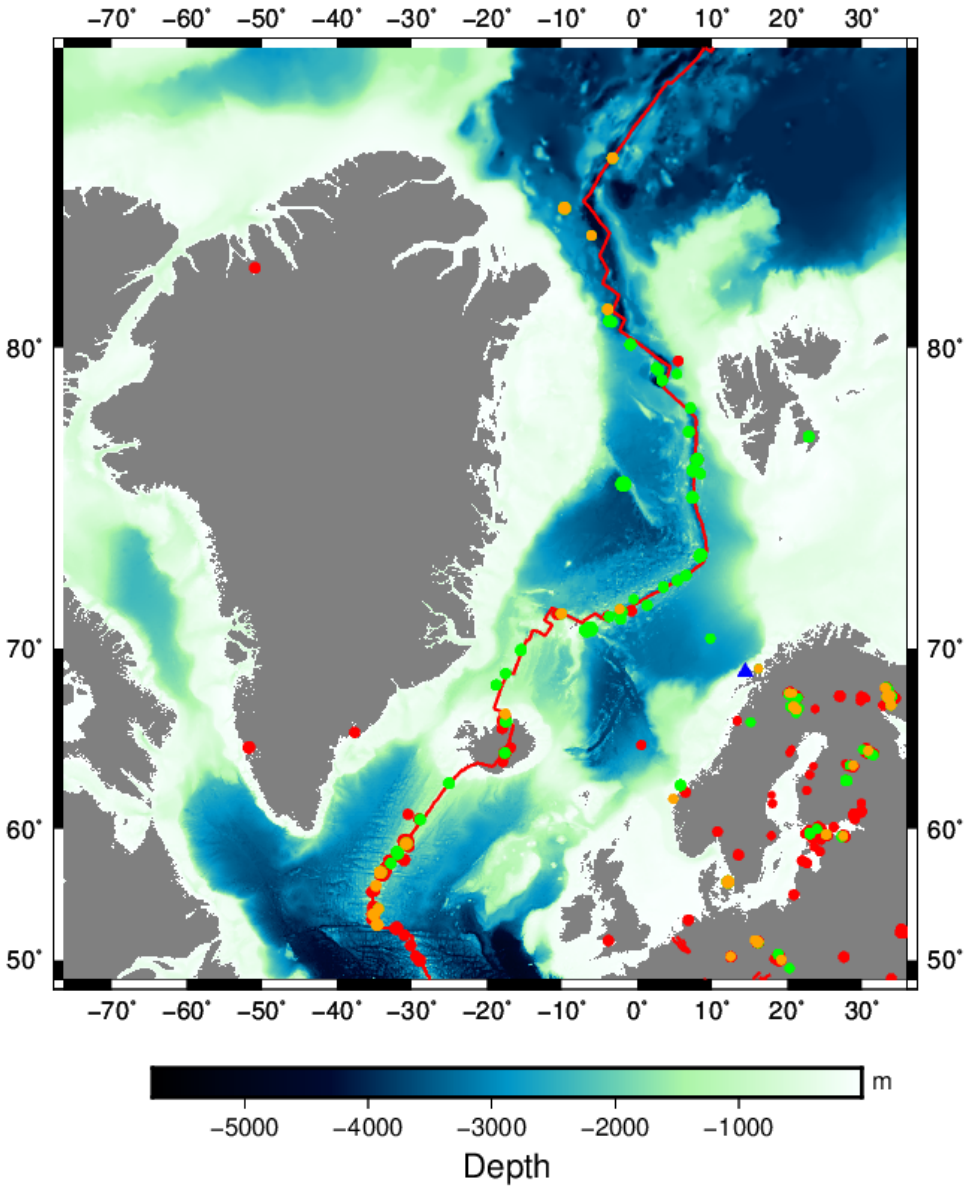

Figure 6: Distribution of detected and undetected earthquakes from the LoVe observatory. Green spots represent earthquakes with multiple corresponding arrivals in the LoVe data, Orange spots represent single arrivals, and red spots have no corresponding arrival. The earthquake spots are scaled so that larger magnitude earthquakes are represented by larger diameter spots. The red line represents the Mid-Atlantic Ridge, and the bathymetry data is from GEBCO.[14]

An earthquake was considered detected if the signal appeared in the LoVe data within $\pm 10\%$ of the predicted travel time. For the seismic arrivals, this reflected a reasonable variance in travel time residuals for the area.[19] Acoustic travel time of the earthquake through the water column was straightforward to calculate, but the seismic travel time through the solid earth required some additional steps. The open-source software TauP[11] was used as a seismic phase travel time calculator. The required input parameters for the calculation included the geodesic distance between the earthquake epicentre and the LoVe hydrophone, and the depth of the epicentre. This depth was chosen as a fixed 0 km as much of the depth data is not reported on the ISC[18] database, and changing the depth by up to 10 km at a time was found to impact the resulting arrival

time predictions by less than one second, which would be highly unlikely to cause the prediction to fall outside of the 10% error window. Locations of the 62 earthquakes that were detected in 2018 are shown in Fig. 6. The detected earthquake magnitudes (m_b) ranged between 2.5 and 4.9, at source-to-station distances ranging from 73 km to 2212 km. 56% of the 1090 earthquakes from the ISC bulletin fell within periods when the hydrophone was not recording, and a further 29% of ISC events did not have any corresponding signal at LoVe. Approximately 20% of the remaining earthquakes were detected at LoVe either as single arrival events, or multiple arrival events, but outside of the 10% error window, leaving 5% of the arrivals falling within the error window. Although not discussed here, an additional seismic bulletin[25] that contains earthquakes of magnitudes down to -1.98 has been collected, and the signals that fall outside of the error window will be cross-referenced.

Possible reasons that some earthquakes were detected whilst others, especially if from similar locations were not, could involve different earthquake magnitudes, different paths of propagation, and the sound levels at LoVe. The acoustic signal of earthquakes of a magnitude of 2 or less are unlikely to propagate as far as a larger magnitude earthquake,[30] and the propagation paths from some geological regions may mean that a signal is far less likely to reach LoVe. For example, the region of the Mid-Atlantic Ridge to the south of Iceland appears to be a location from which an earthquake signal rarely appears at LoVe. As can be seen in the bathymetry of Fig. 6, this coincides with two large fracture zones - the Charlie-Gibbs and the Bight Fracture Zones. Fractured rock results in delays in the acoustic propagation, and reduces the signal amplitude,[4] so it is unsurprising that the earthquakes from this geological setting mostly went undetected at LoVe. Other possible explanations for undetected events could involve the bathymetry between the epicentre and LoVe - for example, in Fig. 6 a bathymetric high (the Rockall Rise) is visible to the northwest of the U.K., and presents a possible barrier to some events originating south of Iceland - but to determine this, thorough testing of propagation models would be necessary. Other explanations for undetected earthquakes at LoVe also include a rise in local ambient noise, as a result of a storm for instance, or that the arrival coincides with a masking transient noise at LoVe like shipping.

BROADBAND SOUND PRESSURE LEVEL AND FREQUENCY BANDS

Fig. 7 shows an example of how the SPL varied over the course of one day in winter. In Fig. 7A a clear peak at 20 Hz is visible. This corresponds to the 20 Hz fin whale calls - February is within breeding season when this particular call is most common, and when the signal peaks in intensity. There is also a small degree of undulation in the median line of the box plots further up the frequency range. Each small peak aligns with a faint tonal line from distant or brief signals from shipping. In Fig. 7B there is more detail to be seen, with the most obvious peak in broadband SPL occuring at sunset, with smaller peaks about one hour and two hours preceding sunrise, as well as some peaks following the sunrise. These are likely to be due to biological activity, most likely fish movements.[9]

Over the period of a month, the undulating trend seen in the frequencies over 20 Hz in Fig.7A flatten out as the amount of shipping noise and tonal lines of different vessels average out. The height of the peak at 20 Hz varies with season - being much more prominent in winter months versus summer months. The peak in broadband SPL that typically occurs just before sunrise and sunset reduce when averaged over a month, but in months where the number of daylight hours do not change too much (by an hour or less), they remain present. The 20 Hz peak is visible in every month of the year, but is most prominent within the winter months, or fin whale breeding season in the northern hemisphere.

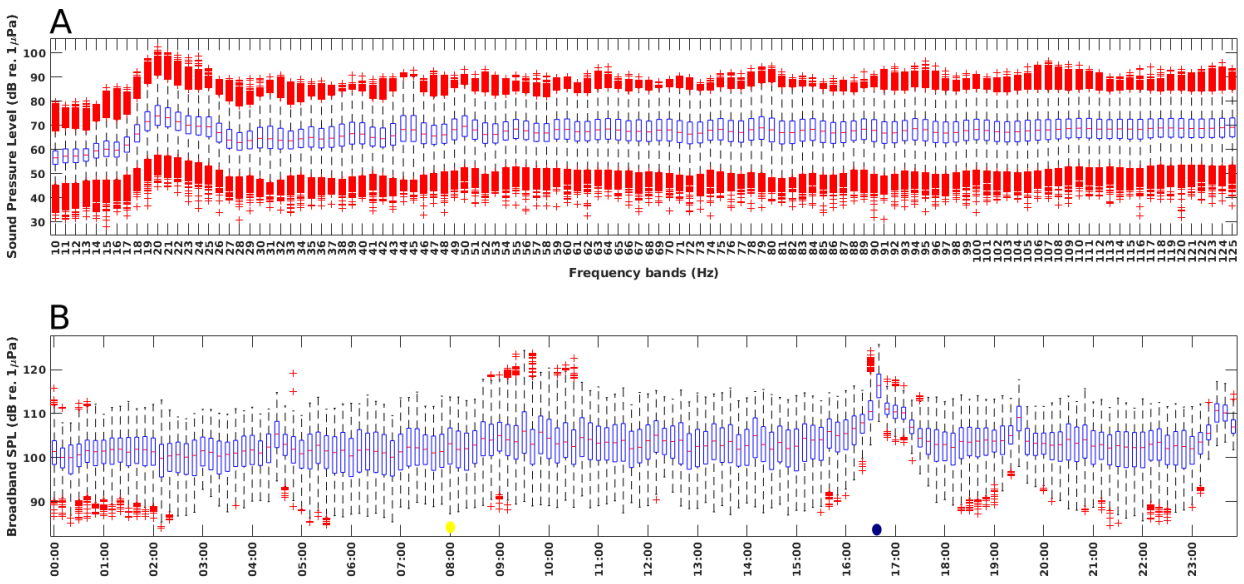

Figure 7: A: Sound pressure level variation over frequency bands from 10 Hz to 125 Hz over 21st February 2018. B: Broadband sound pressure level variation over the course of 21st February 2018. The yellow and blue circles represent the time of sunrise and sunset respectively.

CONCLUSION

In the LoVe dataset daily shipping signals were found, with insightful features like LME interference patterns, which can be used to determine CPA, and even track vessel movements.[35,36] Wind signals were found - with spectrum saturation occurring during periods of high wind speed. There were also instances where wind speed and broadband SPL (see Figure 5) showed no correlation at all. It was concluded that broadband SPL was too crude a measurement of wind speed, and that factors like fetch, constancy of wind, direction in relation to currents, swells, and nearby topography should also be taken into account.[8,33] The most common biological source identified in the LoVe data was from a fin whale - specifically the "20 Hz call" male fin whales make during breeding season. Strong seasonal variation in whale vocalisations was observed, with the 20 Hz call peaking in frequency and intensity during the winter months (breeding season), and the higher frequency calls were more commonly observed in spring. 62 earthquakes were verified by their seismic and water phases, with epicentres ranging as far as 2212 km away from LoVe. Possible reasons for unverified events include geological setting (earthquakes originating from a transfer zone are less likely to propagate as efficiently), bathymetry that results in a propagation path of high transmission loss, that the arrivals coincided with periods of high ambient noise, like wind, or a high transient noise, like shipping, or that the manually-found signals actually correspond to more local, lower magnitude events.

ACKNOWLEDGEMENTS

This research is supported by the UK Engineering and Physical Sciences Research Council (EPSRC), as part of industrial Cooperative Award in Science and Technology (iCASE) project #2279119, supported by Defence Science & Technology Laboratory (Dstl) and AWE Forensic Seismology.

REFERENCES

[1] C. Audoly, V. Meyer, "Measurement of radiated noise from surface ships - Influence of the sea surface reflection coefficient on the Lloyd's mirror effect", Proceedings of ACOUSTICS 2017 Perth: Sound, Science and Society, **Section 3**, 1–10 (2017).

[2] M. G. Aulich, R. D. McCauley, D. Robert, B.J. Saunders, M.J.G. Parsons, "Fin whale (Balaenoptera physalus) migration in Australian waters using passive acoustic monitoring", *Nature Scientific Reports*, **9**, 1–12 (2019).

[3] D. K. Blackman, C. E. Nishimura, J. A. Orcutt, "Seismoacoustic recordings of a spreading episode on the Mohns Ridge", *Journal of Geophysical Research: Solid Earth*, **105:B5**, 10961–10973 (2000).

[4] F. K. Boadu, L. T. Long, "Effects of fractures on seismic-wave velocity and attenuation", *Geophysical Journal International*, **12:1**, 86-110 (1996).

[5] R. Bøe, V. K. Bellec, M. F. J. Dolan, P. Buhl-Mortensen, L. Buhl-Mortensen, D. Slagstad, L. Rise, "Giant sandwaves in the Hola glacial trough off Vesterålen, North Norway", *Marine Geology* **267:1**, 36–54 (2009).

[6] S. J. Buchan, L. Gutierrez, N. Balcazar-Cabrera, K. M. Stafford, "Seasonal occurrence of fin whale song off Juan Fernandez, Chile", *Endangered Species Research*, **39:1998**, 135–145 (2019).

[7] D. H. Cato, "Theoretical and measured underwater noise from surface wave orbital motion", *Journal of the Acoustical Society of America*, **89:3**, 1096–1112 (1991).

[8] P. Cauchy, K. J. Heywood, N. D. Merchant, B. Y. Queste, P. Testor, "Wind speed measured from underwater gliders using passive acoustics", *Journal of Atmospheric and Oceanic Technology*, **35:12**, 2305–2321 (2018).

[9] P. A. Ching, D. E. Weston, "Wideband studies of shallow-water acoustic attenuation due to fish", *Journal of Sound and Vibration*, **18:4**, 499-510 (1971).

[10] D. A. Croll, C. W. Clark, A. Acevedo, B. Tershy, S. Flores, J. Gedamke, J. Urban, "Only male fin whales sing loud songs", *Nature*, **417:6891**, 809–809 (2002).

[11] H. P. Crotwell, T. J. Owens, J. Ritsema, "The TauP Toolkit: Flexible seismic travel-time and ray-path utilities", *Seismological Research Letters*, **70**, 154-160 (1999).

[12] R. P. Dziak, D. R. Bohnenstiehl, H. Matsumoto, C. G. Fox, D. K. Smith, M. Tolstoy, T. K. Lau, J. H. Haxel, M. J. Fowler, "P- and T-wave detection thresholds, Pn velocity estimate, and detection of lower mantle and core P-waves on ocean sound-channel hydrophones at the Mid-Atlantic Ridge", *Bulletin of the Seismological Society of America*, **94:2**, 665–677 (2004).

[13] A. Farcas, C. F. Powell, K. L. Brookes, N. D. Merchant, "Validated shipping noise maps of the Northeast Atlantic", *Science of the Total Environment*, **735**, 139509 (2020).

[14] GEBCO Compilation Group (2020) GEBCO 2020 Grid (doi:10.5285/a29c5465-b138-234d-e053-6c86abc040b9)

[15] O. R. Godø, S. Johnsen, T. Torkelsen, "The LoVe ocean observatory is in operation", *Marine Technology Society Journal* **48:2**, 24–30 (2014).

[16] J. H. Haxel, R. P. Dziak, P. Robert, H. Matsumoto, "Observations of shallow water marine ambient sound: The low frequency underwater soundscape of the central Oregon coast", *The Journal of the Acoustical Society of America*, **133:5**, 2586-2596 (2013).

[17] F. Igenito, S. N. Wolf, "Site dependence of wind-dominated ambient noise in shallow water", *Journal of the Acoustical Society of America*, **85:1**, 141-145 (1989).

[18] International Seismological Centre, Online Bulletin, https://doi.org/10.31905/D808B830 (2020).

[19] A. L. Levshin, J. Scweitzer, C. Weidle, N. M. Shapiro, M. H. Ritzwoller, "Surface wave tomography of the Barents Sea and surrounding regions", *Geophysical Journal International*, **170:1**, 441-459 (2007).

[20] M. S. Longuet-Higgins, "A Theory of the Origin of Microseisms", *Philosophical Transactions of the Royal Society of London*, **243:857**, 2–35 (1950).

[21] M. F. McKenna, D. Ross, S. M. Wiggins, J. A. Hildebrand, "Underwater radiated noise from modern commercial ships", *The Journal of the Acoustical Society of America*, **131**, 92–103 (2012).

[22] N. D. Merchant, K. M. Fristrup, M. P. Johnson, P. L. Tyack, M. J. Witt, P. Blondel, S. E. Parks, "Measuring Acoustic Habitats", *Methods in Ecology and Evolution*, **2041-210X.12330** (2015).

[23] Metas, "Ocean Observatory Vesterålen", Statoil, URL: https://love.statoil.com/Resources/LoVe%20Ocean%20Observatory%20Sensor%20System.pdf (2014)

[24] J. L. Morano, D. P. Salisbury, A. N. Rice, K. L. Conklin, K. L. Falk, C. W. Clark, "Seasonal and geographical patterns of fin whale song in the western North Atlantic Ocean", *The Journal of the Acoustical Society of America*, **132:2**, 1207–1212 (2012).

[25] NORSAR, "Seismic Bulletins", https://www.norsar.no/seismic-bulletins/, (2020), Accessed on: 23-05-2020.

[26] L. Ødegaard, G. Pedersen, E. Johnsen, "Underwater Noise from Wind at the High North LoVe Ocean Observatory", *UACE 2019 Conference Proceedings*, 359–366 (2019).

[27] A. Pereria, D. Harris, P. Tyack, L. Matias, "Lloyd's mirror effect in fin whale calls and its use to infer the depth of vocalizing animals", *Proceedings of Meetings on Acoustics*, **27**, 070002, (2016).

[28] C. L. Piggott, "Ambient Sea Noise at Low Frequencies in Shallow Water of the Scotian Shelf", *The Journal of the Acoustical Society of America*, **36:11**, 2152-2163 (1964).

[29] S. Sauer, A. Crémière, J. Knies, A. Lepland, D. Sahy, T. Martma, S. R. Noble, J. Schönenberger, M. Klug, C.J. Schubert, "U-Th chronology and formation controls of methane-derived authigenic carbonates from the Hola trough seep area, northern Norway", *Chemical Geology* **470**, 164–179 (2017).

[30] P. D. Slack, C. G. Fox, R. P. Dziak, "P wave detection thresholds, Pn velocity estimates, and T wave location uncertainty from oceanic hydrophones", *Journal of Geophysical Research: Solid Earth*, **104:B6**, 13061–13072 (1999).

[31] T. Van England, O. R. Godø, E. Johnsen, G. C. A. Duineveld, D. van Oevelen, "Cabled ocean observatory data reveal food supply mechanisms to a cold-water coral reef",*Progress in Oceanography*, **172**, 51–64 (2019).

[32] S. C. Wales, R. M. Heitmeyer, "An ensemble source spectra model for merchant ship-radiated noise", *The Journal of the Acoustical Society of America*, **111:3**, 1211–1231 (2002).

[33] G. M. Wenz, "Acoustic ambient noise in the ocean: spectra and sources", *The Journal of the Acoustical Society of America*, **34:12**, 1936–1956 (1962).

[34] W. S. D. Wilcock, K. M. Stafford, R. K. Andrew, R. I. Odom, "Sounds in the Ocean at 1—100 Hz", *Annual Review of Marine Science*, **6**, 117–140 (2014).

[35] M. J. Wilmut, N. R. Chapman, G. J. Heard, G. R. Ebbeson, "Inversion of Lloyd mirror field for determining a source's track", *IEEE Journal of Oceanic Engineering*, **32:4**, 940–947 (2007).

[36] J. K. Wilson, "Maritime Surveillance Using a Wideband Hydrophone", *Naval Postgraduate School, Monterey, California* (2007).

[37] G. Zhang, T. N. Forland, E. Johnsen, G. Pedersen, H. Dong, "Measurements of underwater noise radiated by commercial ships at a cabled ocean observatory", *Marine Pollution Bulletin*, **153**, 110948 (2020).